



Research Article

Performance analysis of adsorption refrigeration system using silicagel/methanol pair: experimental & analytical approaches

Palash SONI^{1,*}, Vivek Kumar GABA¹

¹Department of Mechanical Engineering, National Institute of Technology, Raipur, India

ARTICLE INFO

Article history

Received: 20 July 2019

Accepted: 11 September 2019

Key words:

Adsorption refrigeration; Silica-gel/Methanol; Thermal compressor; Thermal gravimetric analysis; Exhaust heat

ABSTRACT

An adsorption refrigeration system (ARS) working on silica-gel/methanol pair has been investigated analytically and experimentally. By applying the mass balance in the adsorber bed the mechanism of adsorption in the thermal compressor with respect to time and bed length was determined. An experimental analysis was performed using a thermal gravimetric analyzer (TGA) to evaluate the mass transfer coefficient and optimum cycle time for silica-gel/methanol pair at different working temperatures. The Diffusion coefficient D_s and Activation energy E_a for silica-gel/methanol pair were found $2.55 \times 10^{-4} \text{ m}^2/\text{s}$ and 83.08 KJ/mol . Further, the results of variation of regeneration temperature on the performance of the system in terms of COP (Coefficient of Performance) and SCP (Specific Cooling Power) was evaluated; the maximum average theoretical COP and SCP achieved by the system was 0.5 and 102 W/kg near about 127°C regeneration temperature.

Cite this article as: Soni P, Gaba VK. Performance analysis of adsorption refrigeration system using silicagel/methanol pair: experimental & analytical approaches. J Ther Eng 2021;7(5):1079–1089.

INTRODUCTION

The adsorption refrigeration technology uses a low grade of energy (Heat) instead of a high grade of energy (Work) for refrigeration purposes. Since the refrigerant used in the system is eco-friendly and natural refrigerants like water, ammonia, and methanol can be used for refrigeration, it makes this system suitable for the future era.

Another advantage is that these systems do not require electricity, which solves the problem for those areas where electricity is either not available or not reliable. The disadvantage associated with ARS is that this system comprises more components as compared to vapour compression system (VCS). In addition, debris resulting from the corrosion fouls narrow down the openings in the system.

*Corresponding author.

*E-mail address: psoni.phd2017.mech@nitrr.ac.in, vgaba.mech@nitrr.ac.in

This paper was recommended for publication in revised form by Regional Editor Siamak Hoseinzadeh



In a conventional VCS, the compressor is a major part of the system, which is used to compress the refrigerant from evaporator pressure to condenser pressure and also continue to circulate the refrigerant through the refrigerating system. In a similar manner, a unit that performs the same function as a conventional compressor but utilizes heat energy in the sorption system is known as a thermal compressor.

The researcher found that the heat transfer rate in thermal adsorber bed is very poor; this is because of low thermal conductivity of adsorbent, inefficient design of adsorber bed, and low heat transfer coefficient between the heat transfer fluid and adsorber bed walls. There are few ways to enhance heat transfer.

- By mixing the metal powder and metal foam.
- By making the composite of adsorbent using expanded natural graphite, activated carbon fibre, CaCl_2 etc.
- Improving the design of adsorber bed, which provides more surface area for heat transfer like spiral plate, fined tube type adsorber bed.
- Reducing the thermal contact resistance between wall and adsorbent (using coated adsorber bed)
- By using the heat pipes in the adsorber bed to improve the heat transfer.

At the beginning of the 2000s, Chua et al. [1] experimentally analysed the adsorption characteristics of pure water vapour with two different types of silica-gel in the range of temperature 25°C to 65°C and at different equilibrium pressure range between 500 to 7000 Pa using a volumetric technique. Freni et al. [2] presented an ARS for cold storage using solar energy for regeneration. They used ethanol as a working fluid instead of methanol due to its less toxic and corrosive nature and obtained a COP of 0.1. Skoda and Suzuki [3] presented some fundamental experimental and theoretical studies which were carried out for silica-gel/water working pair. Berdja et al. [4] represented an experimental model that adopted an adsorption tube collector for refrigeration. The thermal COP obtained is 0.49 and the solar COP obtained is 0.081. Liu et al. [5] built up an ARS working on silica-gel/water pair without using any refrigerant valves. This component decreased the expense of the system and made it progressively solid as there are fewer movable parts that could permit air invasion.

Zhong et al. [6] proposed an air conditioning system based on adsorption technology for a heavy-duty truck. The system works on Zeolite/water pair using the exhaust heat of the diesel engine as a prime heat source. It is observed that the COP varies in the range of 0.23 to 0.498 and SCP in the range of 40 W/kg to 125 W/kg. Saha et al. [7] performed an experimental analysis on a double-stage, four-bed, non-regenerative ARS using solar/waste heat sources in the range of 50°C and 70°C . Nunez et al. [8] prepared and examined a silica-gel/water ARS with a purported cooling power of 3.5 kW. Saha et al. [9] studied adsorption capacity

of ethanol into a pitch-based activated carbon fibre (ACF) of type (A-20). Direct adsorption capacity, as well as the adsorbent temperature, is observed with the help of a thermal gravimetric analyzer (TGA) unit. Chin Ni et al. [10] played out an estimation of the clear solid-side mass diffusivity of water fume adsorbed in a normal thickness silica gel by utilizing a constant-pressure TGA. Hamdeh et al. [11] performed an experimental analysis to optimize the design parameter of the solar ARS. The minimum temperature of 9°C was observed in the evaporator corresponding to the atmospheric temperature of 26°C . Deshmukh et al. [12] presented a new design of ARS in which three adsorber bed (two identical small and one big) was used this system attain an average COP and SCP of 0.63 and 337.5 kJ/kg respectively. Sur et al. [13] developed simple equilibrium and dynamic models which can be used for generating simulation results of different combinations of adsorbate and adsorbent. Sheikholeslami et al. [14] [15] investigates the impact of using fins and nano-sized materials on the performance of the discharging system. Dixit et al. [16] presented the waste heat driven triple effect refrigeration cycle from the viewpoint of both energy and exergy concepts of thermodynamics. Javadi et al. [17] reproduced an ordinary consolidated cycle power age unit in Iran by a numerical strategy to perform an affectability examination on climate discharge and power cost. Sheikholeslami et al. [18] [19] explained various ways of heat transfer enhancement in a heat exchangers using nanofluids. Kurtulmus et al. [20] modelled and analysed a Vapour Absorption cooling system; this system utilised the waste heat from the exhaust gases of the I.C. engine of a passenger bus. This system is used for the air conditioning of the driver cabin with different working conditions. Kalla et al. [21] performed a comparative analysis between different refrigerants such as R22, R407C, R432A, R438A and NM1 (R32/R125/R600a) to obtain a perfect replacement of HCFC 22 for refrigeration purposes. Javadi et al. [22] introduced a joined cycle power plant with an ostensible limit of 500 MW, the examination is done to enhance three target elements of exergy efficiency, CO_2 emanation and created power costs. Anand et al. [23] performed the energy and exergy analysis on an absorption refrigeration system which is used for the air conditioning purpose of a residential building. In this system, the solar energy is used for regeneration purpose. Bhargav et al. [24] developed an ARS system working on activated carbon/methanol pair using the solar energy for regeneration. This system is used for food preservation and they produced a cooling effect of 554 kJ in 6 hours in 10 kg of water.

Only a few people work on the design of an adsorber bed using the mass transfer analysis, in this article many concepts have been covered. The main aim is to promote quick, reasonably, reliable design by taking into account the most important properties of adsorbent: capacity, kinetics, bed dynamics, and adsorption dynamics, etc. because of the simplification and idealisation there are many factors

that could not be addressed. Moreover, there are only a few researchers found that sheds light on that type of adsorption system which is operated using the waste heat of the I.C. engine.

As water cannot be used as a refrigerant for those applications where the sub-zero temperature is required to attend, so a silica-gel/methanol pair has gained importance. Due to the lower freezing temperature of methanol as compared to water, it can be used as a working fluid for thermally driven refrigeration system therefore, it was decided to investigate the ideal performance of an engine exhaust-driven silica-gel/methanol-based ARS, using the approach of Skoda et al. [3] and the result is presented in this paper.

SYSTEM DESCRIPTION

An ARS utilizes heat energy instead of mechanical work, so conventional compressor has to be replaced by a thermal compressor. A proposed thermal system for silica-gel/methanol pair is shown in Figure (1).

In this system silica-gel is used as an adsorbent and methanol is used as an adsorbate. This system consists of two cylindrical vessels completely filled with silica-gel and methanol. Inside the cylindrical vessel, a concentric copper tube is placed for circulating hot and cold water throughout the adsorber bed respectively for heating and cooling the silica-gel. The silica-gel, when cooled, adsorb the methanol and when heated, desorbs it. The two adsorber bed is used for the continuous cooling operation.

In this system, the adsorber bed utilizes the heat energy of hot water, which is taking the heat of exhaust of the I.C. engine by passing through a heat exchanger. In the first phase of operation, the hot water is circulated through adsorber bed I and cooling water is circulated through bed II. Also in this phase, valves V_1 and V_4 are kept closed and V_2 and V_3 are kept open. Similarly, during the second phase hot water is circulated through adsorber bed II and cold water is circulated through adsorber bed I, to achieve desorption in adsorber bed II and adsorption in bed I. During the second phase valves, V_1 and V_4 are kept opened and V_2 and V_3 are kept closed.

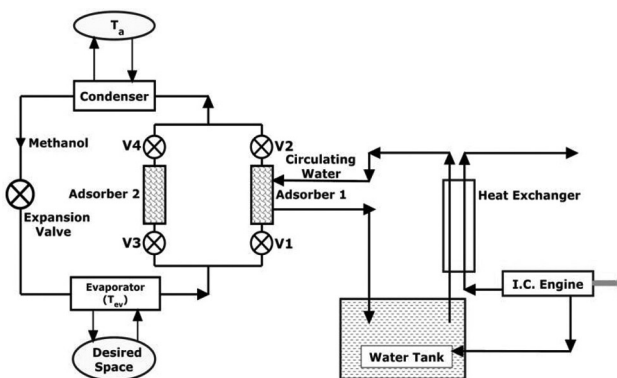


Figure 1. Schematic diagram of the system.

With the help of two adsorber beds, this system is able to produce a continuous cooling effect. The cycle refreshes the same thing in a manner like the VCS by alternating the circulation of hot water and cold water in the adsorber bed I and adsorber bed II respectively. During desorption superheated methanol is released at the pressure of the condenser i.e. P_{cond} in the same manner as in VCS. After that, the methanol is condensate at a temperature T_{cond} in the condenser by rejecting the heat to the ambient at a temperature T_a . Subsequently, it goes through an expansion valve, thus lowering the pressure to P_{ev} . This methanol at low pressure and low temperature is evaporated at T_{ev} by taking the heat from the evaporator.

METHODOLOGY

Analysis of Adsorber Bed

The mechanism of adsorption in the adsorber bed is shown in Figure (2). Adsorber bed is packed with silica-gel, low-pressure methanol from the evaporator enters it and the maximum mass is adsorbed by silica-gel, a few of it is in pores and dead volume. The dead volume is the small zones within the adsorber bed where some methanol molecules are trapped without any participation in the refrigeration process. So applying the mass balance in the bed,

$$(M_{METH})_{IN} - (M_{METH})_{OUT} = (M_{METH})_{ADS} + (M_{METH})_{PORES} + (M_{METH})_{DEAD}$$

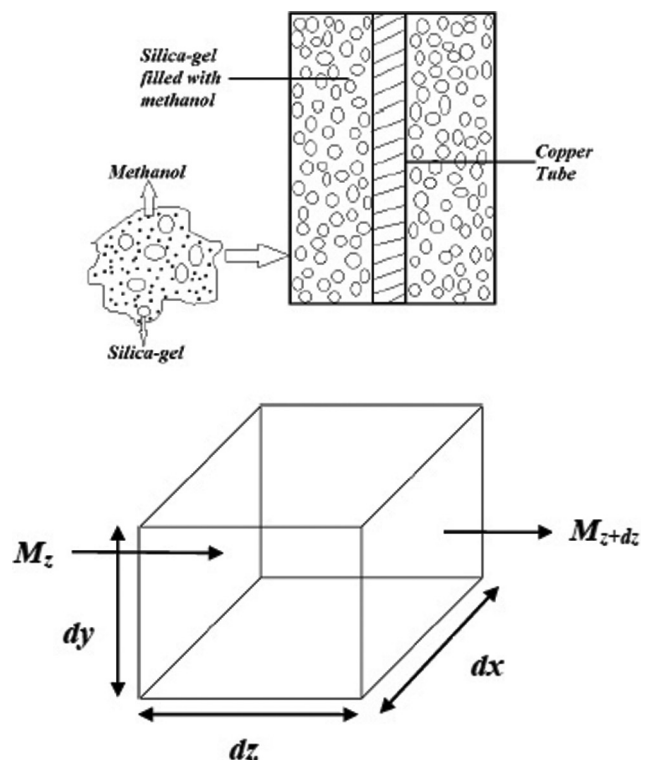


Figure 2. Sectional view of the bed and elemental volume of adsorber bed.

Now for an infinitesimal volume in the bed

$$(M_{METH})_{IN} - (M_{METH})_{OUT} = \left[\left(\dot{M}_z + \frac{\partial \dot{M}_z}{\partial z} dz \right) - \dot{M}_z \right] dx dy \quad (1)$$

Where \dot{M}_z represents the mass flow rate per unit area in the Z direction

$$\text{And } \dot{M}_z = D_s \frac{\partial C}{\partial z}$$

$$(M_{METH})_{IN} - (M_{METH})_{OUT} = D_s \frac{\partial^2 C}{\partial z^2} dx dy dz \rho_b$$

The mass of methanol adsorbed in the element volume is given by

$$(M_{METH})_{ADS} = \rho_b \frac{\partial n}{\partial t} dx dy dz$$

The mass of methanol accumulated in the pore volume is given by

$$(M_{METH})_{PORES} = \rho_b (\varepsilon_p dx dy dz) \frac{\partial C}{\partial t}$$

where $(\varepsilon_p dx dy dz)$ is pore volume

$$(M_{METH})_{DEAD} = \rho_b (\varepsilon_p dx dy dz) v \frac{\partial C}{\partial t}$$

Where v is the interstitial velocity

Substituting all these values in Equation (1)

$$\rho_b \frac{\partial n}{\partial t} + \rho_b \varepsilon_p \frac{\partial C}{\partial t} + \rho_b \varepsilon_p v \frac{\partial C}{\partial z} = D_s \frac{\partial^2 C}{\partial z^2} \rho_b \quad (2)$$

At the break through point, $(M_{METH})_{IN} = (M_{METH})_{OUT}$ hence Equation (2) yields

$$\frac{\partial n}{\partial t} + \varepsilon_p \frac{\partial C}{\partial t} + \varepsilon_p v \frac{\partial C}{\partial z} = 0 \quad (3)$$

Let $V_s = \varepsilon_p v$ then Equation (3) changes to

$$\frac{\partial n}{\partial t} + \varepsilon_p \frac{\partial C}{\partial t} + V_s \frac{\partial C}{\partial z} = 0$$

For a small change in amount adsorbed i.e. Δn , equation can be rearranged as

$$\frac{\partial z}{\partial t} \left[\frac{\partial n}{\partial z} + \varepsilon_p \frac{\partial C}{\partial t} \right] = -V_s \frac{\partial C}{\partial z} \quad (4)$$

The step velocity V is defined as

$$V = -\frac{\partial z}{\partial t} \text{ Hence Equation (4) yields}$$

$$V = \left(\frac{V_s}{\varepsilon_p + \frac{\partial n}{\partial C}} \right)$$

From Henry's law $n = HC$, hence equation may be written as

$$V = \left(\frac{V_s}{\varepsilon_p + H} \right)$$

If L be the length of cylinder and t^* be the equilibrium time for the adsorption, then the step velocity V is $V=L/t^*$ therefore t^* is expressed as

$$t^* = \frac{L(\varepsilon_p + H)}{V_s} \quad (5)$$

Further if Q is the flow rate of methanol and V_{ads} be the volume of the adsorber bed, and then Equation (5) gives

$$t^* = \frac{V_{ads}(\varepsilon_p + H)}{Q}$$

Now using Henry's law, Equation (3) reduces to

$$A_1 \frac{\partial^2 n}{\partial z^2} + A_2 \frac{\partial n}{\partial z} + A_3 \frac{\partial n}{\partial t} = 0 \quad (6)$$

$$\text{Where } A_1 = -\frac{D_s}{\rho_b}, A_2 = V_s = \frac{Q}{A}, A_3 = (H + \varepsilon_p) = \frac{t^* Q}{V_{ads}}$$

Using separation of variables, solution of Equation (6) with $n(z,t) = f(z)g(t)$, gives

$$A_1 \frac{f''(z) - A_2 f'(z)}{f(z)} = A_3 \frac{g'(t)}{g(t)} = \lambda$$

By solving and taking $\lambda = -1$ for without any loss of generality, one gets

$$g(t) = C_1 e^{-\frac{1}{A_3 t}} \text{ And } f(z) = C_2 e^{\mu_1 z} + C_3 e^{\mu_2 z}$$

$$\text{where } \mu_{1,2} = \frac{-A_2 \pm \sqrt{A_2^2 - 4A_1}}{2A_1}$$

Hence the solution of Equation (6) is given by

$$n(z,t) = e^{-\frac{t}{A_3}} (C_2 e^{\mu_1 z} + C_3 e^{\mu_2 z})$$

Now using the initial and boundary conditions

- (i) At $t = 0$ & $z = L$, $n = 0$
- (ii) At $t^* = t$ & $z = 0$, $n = n^*$

The constants are evaluated and equation is finally written as

$$\frac{n}{n^*} = e^{-\left(\frac{1-t}{t}\right) \frac{V_{ads}}{Q}} \left[\frac{e^{\mu_1 z} + e^{\mu_2 z}}{1 - e^{(\mu_2 - \mu_1)L}} \right] \quad (7)$$

The equilibrium amount of adsorption, is proposed by Skoda et al. [3] as

$$n^* = k \left(\frac{p}{p_s} \right)^{1/m} \quad (8)$$

Where k is given by

$$k = \rho^* \left(\frac{\varepsilon_p}{\rho_p} \right)$$

Where, ρ^* for methanol is 800 kg/m³, ε_p for silica-gel is 0.44 and ρ_p for silica-gel is 1300 kg/m³. Hence the value of k for silica-gel/methanol pair is 0.27.

Using Equation (8), methanol per kg of silica-gel desorbed from bed i.e. Δn is evaluated as [3]

$$\Delta n = k \left[\frac{P_s (T_{ev})^{1/m}}{P_s (T_a)^{1/m}} - \frac{P_s (T_{cond})^{1/m}}{P_s (T_{reg})^{1/m}} \right] \quad (9)$$

Experiment Analysis for Determination of Mass Transfer Coefficient $k_s a_p$ for Silica-gel/Methanol Pair

For the performance enhancement of an ARS. The observation of the kinetics of the adsorbent/adsorbate (refrigerant) pair is necessary. However, design and modelling of adsorption processes require the numerical solution of a set of partial differential equations involving time and special variables. The computations can be greatly simplified by using the linear driving force (LDF) method [27]. Customarily, the calculations season of the code could be improved utilizing the notable linear driving force (LDF) relationship. In the LDF technique, the key boundary is the assurance of the overall particle mass transfer coefficient which is can be evaluated by tracking the experimental vapour-uptake behaviour.

Adsorption rate for every adsorbent/adsorbate upon the mass transfer coefficient ($k_s a_p$) of the pair and adsorption rate is given by [3]

$$\frac{dn}{dt} = (k_s a_p) \Delta n \quad (10)$$

where mass transfer coefficient $k_s a_p$ for adsorbent/adsorbate pairs depends upon the physical and chemical properties of the pair and also depends upon the temperature. For evaluating the $k_s a_p$ value for silica-gel/methanol pair Thermal Gravimetric Analyzer (TGA) was used. To make a sample of silica-gel/methanol pair, first of all, methanol was added to silica-gel and left for sufficient time until adsorption had taken place uniformly in the silica-gel. Now a sample of 12.967 mg was taken and placed in a crucible of platinum.

Now this crucible was placed inside the DTG-60 Thermal Gravimetric Analyzer (TGA) in an atmosphere of N₂. The heating rate was adjusted 5°C/min ranging from room temperature to 200°C.

Let W = Equilibrium desorption capacity (kg/kg)
 w = Instantaneous desorption capacity (kg/kg)

Then from Equation (10)

$$\frac{dw}{dt} = k_s a_p (W - w) \quad (11)$$

Let M_T = Total mass of sample

M_s = Mass of silica-gel only (assuming the evaporation of entire methanol)

Then

$$W = \frac{M_T - M_s}{M_s} \quad (12)$$

Similarly, w can also be found out with the help of Equation (12) and Figure (8). So $\frac{dw}{dt}$ value can also be obtained at any time and at any temperature.

Different $k_s a_p$ value at any time and temperature can be evaluated by using Equation (11). $k_s a_p$ is also given by [12]

$$k_s a_p = C_1 \exp(-C_2 / T) \quad (13)$$

Where $C_1 = \frac{15D_s}{R_p^2}$ & $C_2 = \frac{-E_a}{R}$

Hence Equation (13) can also be expressed as

$$\ln(k_s a_p) = C_1 - \frac{C_2}{T} \quad (14)$$

Calculation for SCP and COP of the System

The thermophysical properties of the working fluid methanol are as follows [28]:

Methanol gas characteristic constant given as:

$$\bar{R} = \frac{R}{M_m} = \frac{8.314}{32} = 0.2598 \text{ (kJ / kgK)}$$

Density of liquid methanol can be estimated as:

$$\rho = 920 - 0.0146T - 0.0014 \times T^2 \text{ (kg / m}^3\text{)}$$

Specific heat at constant pressure of methanol vapour is estimated as:

$$C_p(T) = 0.661 + (2.21625 \times 10^{-3} \times T) + (8.09 \times 10^{-7} \times T^2) - (8.90 \times 10^{-10} \times T^3) \text{ (kJ / kgK)}$$

Specific heat at constant volume of methanol vapour is estimated as:

$$C_v(T) = C_p(T) - 0.2598 \text{ (kJ / kgK)}$$

Specific heat of liquid methanol is estimated as:

$$C_{p,f}(T) = (4.38 - 0.0225 \times T) + (6.82 \times 10^{-5} \times T^2) - (4.48 \times 10^{-8} \times T^3) \text{ (kJ / kgK)}$$

Isosteric heat for adsorption:

$$h_{iq} = 4432 \times 0.2598 \times \frac{T}{278} \text{ (kJ / kg)}$$

Isosteric heat for desorption:

$$h_{id} = -4432 \times 0.2598 \times \frac{T}{308} \text{ (kJ / kg)}$$

Enthalpy of saturated vapour of methanol is estimated as:

$$h_g = (-237.75 + 0.0406 \times T) + (0.0048 \times T^2) - (7 \times 10^{-6} \times T^3) \text{ (kJ / kg)}$$

Enthalpy of superheated vapour of methanol is estimated as:

$$h_{sup} = h_g + C_p \times (T - T_{sat}) \text{ (kJ / kg)}$$

Enthalpy of saturated liquid refrigerant is:

$$h_f = -1900.0 + (3.46 \times T) - (0.0062 \times T^2) + (1.0 \times 10^{-5} \times T^3) \text{ (kJ / kg)}$$

In all the equations, temperature T is in kelvin, K.

Refrigeration effect per kg of adsorbent is known as specific cooling power (SCP) of the system now applying energy balance in bed [25]

$$\dot{M}_e C_{pe} (T_e - T_a) \varepsilon = \frac{dn}{dt} M_s [\Delta h_{meth} + E_a] \quad (15)$$

Where $\Delta h_{meth} = (h_g)_{cond} + (C_p)_{meth} (T_{reg} - T_{cond}) - (h_g)_{evp}$ so the refrigeration effect is given by

$$R.E. = \left(\frac{dn}{dt} \right) M_s [(h_g)_{evp} - (h_f)_{cond}]$$

The heat input from I.C. engine exhaust to adsorber bed is

$$H.I. = M_e C_{pe} (T_e - T_a) \varepsilon$$

$$COP = R.E. / H.I. \quad (16)$$

RESULTS AND DISCUSSION

Using Equation (7), the adsorption in the adsorber bed with respect to time as well as the length of the bed was visualised as shown in Figures (3) and (4). In Figure (4) as the adsorption time is increasing more mass of methanol adsorbed but the time required to attend the maximum adsorption i.e. n^* is practically not possible or in other words, it will take infinite time.

Figure (4) shows the variation in adsorption with bed length (z), the adsorption (n) is higher at the entering side of methanol and lowers at the end of the adsorber bed which is due to the layer by layer phenomenon of adsorption. These graphs are important for the design of the adsorber bed.

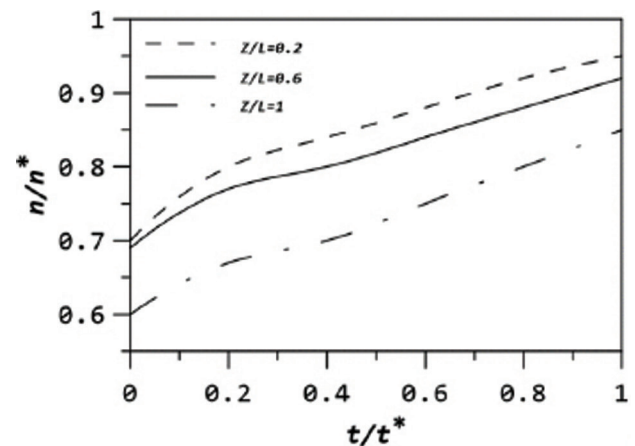


Figure 3. Variation of the adsorbed amount with time.

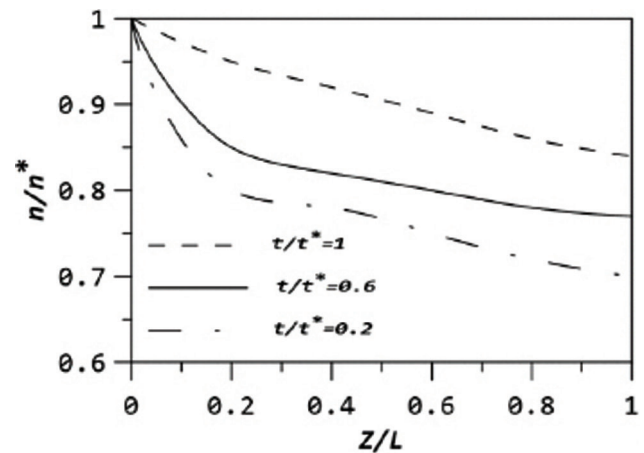


Figure 4. Variation of the adsorbed amount with bed length.

For optimising the value of m , a graph between Δn and m is plotted with different regeneration temperatures T_{reg} , taking evaporator temperature T_{evp} as 7°C , ambient temperature 37°C during peak summer and condenser temperature as 27°C respectively as shown in Figure (5). It is observed that there exists an optimum value of m for each regeneration temperature at which the capacity of adsorption of methanol reaches the maximum. The plot of Δn against m yields an optimum m value for silica-gel/methanol. It is also found that as regeneration temperature is enhanced, Δn also increases due to the increase in saturation pressure corresponding to each regeneration temperature. All curves show maxima at $m = 2$ and therefore m is taken as 2.

Evaporator pressure and condenser pressure are two ranges of pressure between which a thermal compressor is operated. With the help of equation (9) a thermal cycle can be produced as shown in Figure (6), assuming ambient conditions i.e. $T_a = 27^\circ\text{C}$ and $T_{reg} = 97^\circ\text{C}$. Then with the help of Figure (6), Δn can be obtained for the different combination of condenser and evaporator pressure.

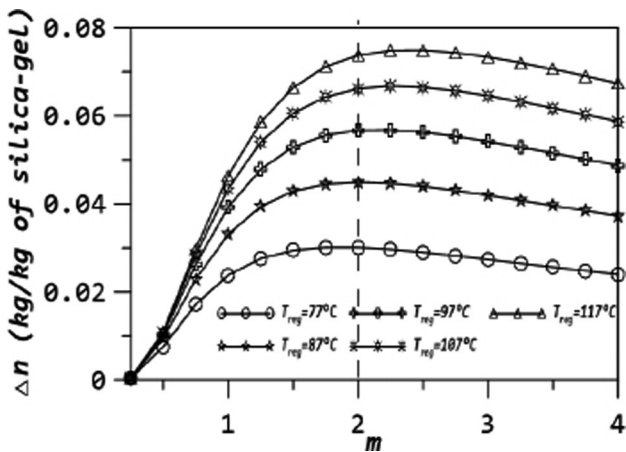


Figure 5. Variation of Δn with parameter m .

TGA was connected to a computer, having the facility of drawing plots between weight vs temperature and weight vs time. The curves obtained are shown in Figure (7) and Figure (8) respectively. It is clear from the Figure 7 and 8 that most of the amount of methanol desorbed up to 120°C near about 16.6 minutes, after that the curves become constant it means that there are no significant outcomes of further increasing the temperature so here we can consider that the optimum desorption time is 16.6 minutes and from literature, we know that the adsorption time is slightly more than desorption time. So the total cycle time (adsorption time + desorption time) for silica-gel/methanol pair can be considered as 35 minutes and the optimum regeneration temperature can be considered as 120°C .

It is clear from Equation (14) that if a curve is plotted between $\ln(k_s a_p)$ vs $1/T$ then both C_1 and C_2 can easily be found, so from Figure (9), the value of C_1 and C_2 are 4.332 sec^{-1} and 3197.9 K/sec , respectively. So Equation (14) becomes

$$\ln(k_s a_p) = 4.332 - (3197.9/T)$$

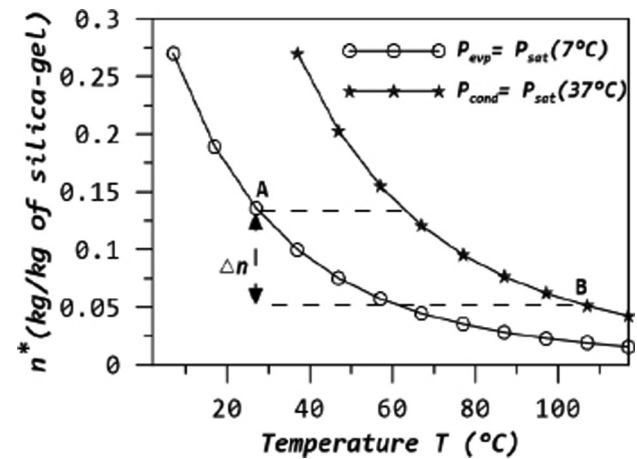


Figure 6. Adsorption cycle between two pressure limit.

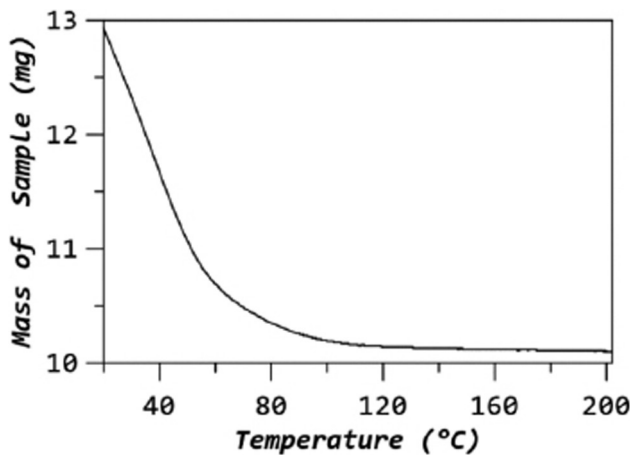


Figure 7. Variation of the mass of sample with temperature.

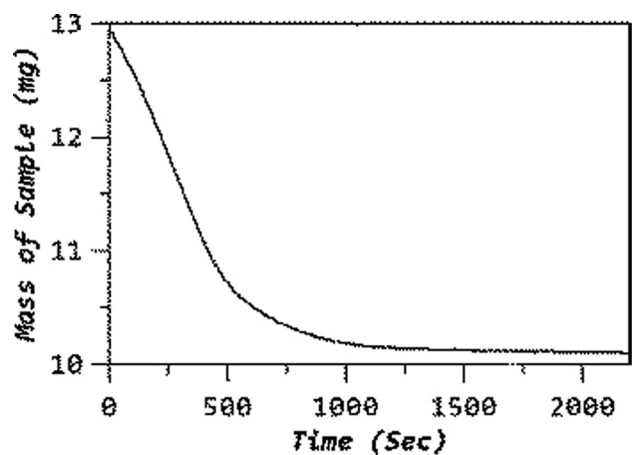


Figure 8. Variation of the mass of sample with time.

Diffusion coefficient D_s and activation energy E_a for silica-gel/methanol pair are calculated as 2.55×10^{-4} m²/s and 83.08 kJ/mol, respectively. Here the size of packed particles of silica-gel is between 8 and 20 meshes and the average radius, R_p is 7.1×10^{-3} m.

A comparison between the experimental value of mass transfer coefficient $k_s a_p$ and the analytical value of $k_s a_p$ identified by using Equation (13) corresponding to different regeneration temperatures is shown in Table 1. From the table, it is observed that the analytical results show a good validation with the experimental research data using the regression dependences. Using Equation (10) & (16), for producing a cooling effect at different evaporator temperatures i.e. 2°C, 7°C and 12°C both SCP and COP of the system were calculated by varying the regeneration temperature from 60°C to 120°C and assuming that ambient

and condenser temperature is 37°C and 27°C, as shown in Figure (10) and Figure (11), respectively.

Both SCP, as well as COP, is the function of regeneration temperature, after minimum regeneration temperature (i.e. the minimum temperature required to run the cycle) both are increasing with regeneration temperature and attaining a maximum value. This is due to the fact that more methanol is desorbed at a higher temperature and passing through the evaporator coil. But after certain regeneration temperature curves become constant because more losses are involved at the elevated temperature.

Uncertainty Analysis

There are a few wellsprings of uncertainty in any TGA analysis. Among these are vacillations in the balance, estimation of temperature by the thermocouple, and test readiness.

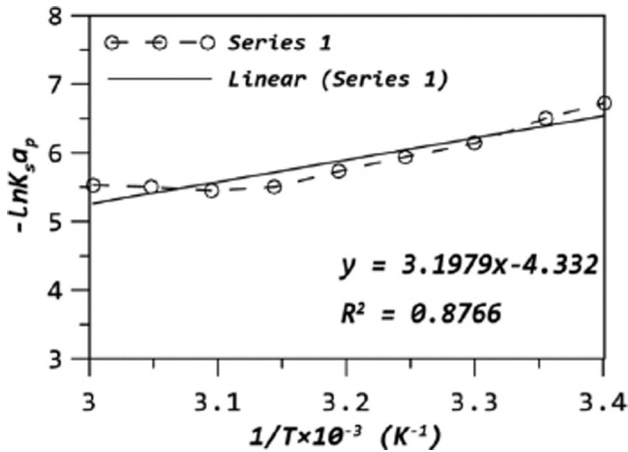


Figure 9. $\ln k_s a_p$ Vs $1/T$.

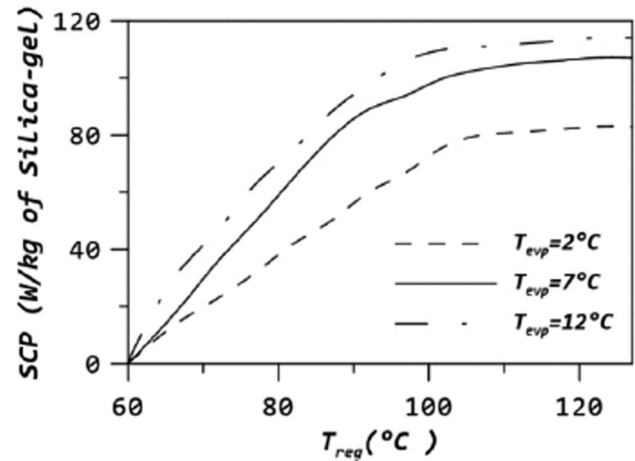


Figure 10. Variation of SCP with T_{reg} .

Table 1. Comparison between experimental and analytical results

S. No.	Temperature (°C)	$k_s a_p$ (Experimentally)	$k_s a_p$ (Analytically)
1	21	1.2×10^{-3}	1.42×10^{-3}
2	25	1.49×10^{-3}	1.64×10^{-3}
3	30	2.16×10^{-3}	2.02×10^{-3}
4	35	2.61×10^{-3}	2.13×10^{-3}
5	40	3.22×10^{-3}	2.68×10^{-3}
6	45	4.04×10^{-3}	3.02×10^{-3}
7	50	4.29×10^{-3}	4.08×10^{-3}
8	55	3.96×10^{-3}	4.38×10^{-3}
9	60	3.95×10^{-3}	4.94×10^{-3}

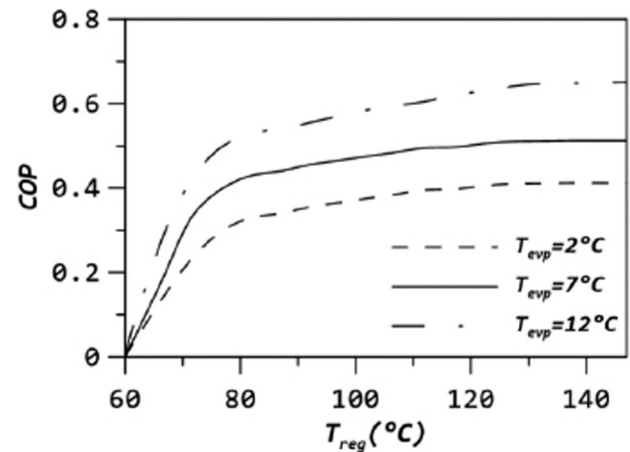


Figure 11. Variation of COP with T_{reg} .

The weight estimations are influenced by vibrations, electricity produced via friction, the thermocouple touching the balance pan, and cleanse gas stream rate. From test preliminaries and different investigations, it was determined that these components are moderately minor and controllable.

The uncertainty in methanol adsorption/desorption uptake measurement (kg/kg⁻¹) based on the TGA test rig. Has been estimated using Equation (17). The experimentally measured adsorption uptake and the corresponding derivatives are also given by Equations (18)-(21) below [25].

$$\delta W = \sqrt{\left(\frac{\partial W}{\partial d} \delta d\right)^2 + \left(\frac{\partial W}{\partial m} \delta m\right)^2 + \left(\frac{\partial W}{\partial h} \delta h\right)^2} \quad (17)$$

$$W = \rho h \frac{\pi}{4} \left(\frac{d^2}{m}\right) \quad (18)$$

$$\frac{\partial W}{\partial d} = \rho h \frac{\pi}{4} \left(\frac{2d}{m}\right) \quad (19)$$

$$\frac{\partial W}{\partial m} = -\rho h \frac{\pi}{4} \left(\frac{d^2}{m^2}\right) \quad (20)$$

$$\frac{\partial W}{\partial h} = \rho \frac{\pi}{4} \left(\frac{d^2}{m}\right) \quad (21)$$

Where δW represent the uncertainty in the methanol adsorption/desorption uptake measurement, δd present the uncertainty of the evaporator diameter and δm is the uncertainty of sample mass measurement whilst δh is the uncertainty in methanol level height measurement using the digital microscope in the TGA experimental test rig. Using Equation (1) the uncertainty of the methanol adsorption/desorption uptake measurement has been found to varying from 4.7% to 5.8%.

Validation of Model

A complete thermodynamic and experimental analysis of ARS working on silica-gel/methanol pair for cold storage was done by Oertel et al. [26]. They developed a laboratory test facility to predict the performance of the system under different working conditions. Table 2 shows a comparison between the COP obtained by Oertel and COP obtained by our numerical equilibrium model with the variation of regeneration temperature. From the table, it was observed that at 75°C regeneration temperature the present numerical model show 4.76% lower COP whereas at 90°C regeneration temperature it shows 3.33% higher COP as compare to Oertel experimental analysis. The variation was found because they used a fined tube type heat exchanger as an adsorber bed and here calculation was done by using a simple cylindrical adsorber bed.

Table 2. Validation of the model

Regeneration Temperature T_{reg} (°C)	COP (obtained by our analysis)	COP (obtained by Oertel [26])	Percentage deviation)
70	0.18	0.20	10% lower
75	0.20	0.21	4.76 % lower
80	0.22	0.23	4.34 % lower
85	0.28	0.27	3.70 % higher
90	0.31	0.30	3.33% higher
95	0.34	0.32	6.25% higher
100	0.37	0.35	5.71% higher

CONCLUSION

A continuous vapour ARS with two adsorber beds powered by the exhaust gases of the I.C. engine has been described. An analytical approach has been used to describe the adsorption phenomenon of methanol into the adsorber bed. The system operates between the lower pressure limit of 0.006 bar and upper pressure of 0.304 bar where the difference in the adsorption uptake Δn could be reached to 0.12 kg/kg of silica-gel. The optimum cycle time for silica-gel/methanol pair was found 35 minutes and the optimum regeneration temperature was found 120°C. It was found that the COP and SCP are the functions of regeneration temperature and as the regeneration temperature increases the COP and SCP also increases, the maximum theoretical COP and SCP achieved by the system at 7°C evaporator temperature was 0.5 and 102 W/kg near about 127°C regeneration temperature. The current work presented research efforts towards the enhancement of silica-gel/methanol adsorption cooling system and it can be considered as a strong foundation for future work. In the future, we can work on the different new composite adsorbents and can work on the development of a new design of adsorber beds to improve the heat and mass transfer performance and the overall efficiency of ARS.

NOMENCLATURE

C	Concentration (mol/mol)
D_s	Diffusivity coefficient (m ² /sec)
$dx dy dz$	Elemental volume (m ³)
E_a	Activation Energy
H	Henry's constant
$ksap$	Temperature dependent mass transfer coefficient
L	Length of adsorber bed (m)
M	Mass of silica-gel and methanol at equilibrium (kg)
M_s	Mass of silica-gel (kg)
MT	Total mass of sample
M_z	Mass flow/unit area in z direction (kg/m ²)

n	Amount adsorbed (kg/kg of silica-gel)
n^*	Equilibrium amount adsorbed (kg/kg of silica-gel)
Δn	Difference of amount adsorbed between before and after regeneration
P	Vapour Pressure
$P_s(T)$	Saturation Vapour pressure at temperature of T
Q	Flow rate (m ³ /sec)
R	Universal gas constant
R_p	Particle radius
T	Temperature (°C)
t	Time (sec)
t^*	Equilibrium time (sec)
V	Step velocity
v	Interstitial velocity
V_s	Superficial velocity
V_{ads}	Volume of adsorber bed
W	Equilibrium desorption capacity (kg/kg)
w	Instantaneous desorption capacity (kg/kg)

Greek symbols

ϵ_p	Pore fraction
ρ	Density (kg/m ³)
ρ^*	Density of adsorbate

Subscripts

a	Ambient
b	Bulk
$cond$	Condensor
evp	Evaporator
$meth$	Methanol
p	Particle
reg	Regeneration
s	Saturation

DATA AVAILABILITY STATEMENT

No new data were created in this study. The published publication includes all graphics collected or developed during the study.

CONFLICT OF INTEREST

The author declared no potential conflicts of interest with respect to the research, authorship, and/or publication of this article.

ETHICS

There are no ethical issues with the publication of this manuscript.

REFERENCES

- [1] Chua HT, Kim CN, Chakraborty A, Nay MO, Mohamed AO. Adsorption Characteristics of Silica Gel + Water Systems. *J. Chem. Eng. Data* 2002;47:1177–1181. <https://doi.org/10.1021/je0255067>.
- [2] Freni A, Santori G, Sapienza A. Solar Powered Solid Adsorption System for Cold-Storage Applications. 16th CIRIAF National Congress. Assisi, Italy. 2016.
- [3] Sakoda A, Suzuki M. Fundamental study on solar-powered adsorption cooling system. *J. Chem. Eng. Japan* 1984;17:52–57. <https://doi.org/10.1252/jcej.17.52>.
- [4] Berdja M, Abbad B, Yahi F, Bouzefour F, Ouali M. Design and realization of a solar adsorption refrigeration machine powered by solar energy. International Conference on Solar Heating and cooling for building and industry. Freiburg, Germany. 2013. <https://doi.org/10.1016/j.egypro.2014.02.139>.
- [5] Liu YL, Wang RZ, Xia ZZ. Experimental study on a continuous adsorption water chiller with novel design. *Int J Refrig.* 2005;28:218–230. <https://doi.org/10.1016/j.ijrefrig.2004.09.004>.
- [6] Zhong Y, Fang T, Wert KL. An adsorption air conditioning system to integrate with the recent development of emission control for heavy-duty vehicles. *Energy* 2011; 36:4125–35. doi.org/10.1016/j.energy.2011.04.032.
- [7] Saha BB, Akisawa A, Kashiwagi T. Solar/waste heat driven two-stage adsorption chiller: the prototype. *Renew. Energy* 2001;23:93–101. [https://doi.org/10.1016/S0960-1481\(00\)00107-5](https://doi.org/10.1016/S0960-1481(00)00107-5).
- [8] Nunez T, Mittelbach W, Henning HM. Development of an adsorption chiller and heat pump for domestic heating and air-conditioning applications. *Appl. Therm. Eng.* 2007;27:2205–2212. <https://doi.org/10.1016/j.applthermaleng.2005.07.024>.
- [9] Saha BB, El-Sharkawy II, Chakraborty A, Koyama S, Yoon SH, Ng KC. Adsorption Rate of Ethanol on Activated Carbon Fiber. *J. Chem. Eng. Data* 2006;51:1587–1592. <https://doi.org/10.1021/je060071z>.
- [10] NiCC, San JY. Measurement of apparent solid-side mass diffusivity of a water vapor–silica gel system. *Int J Heat Mass Transf* 2002;45:1839–1847. [https://doi.org/10.1016/S0017-9310\(01\)00291-5](https://doi.org/10.1016/S0017-9310(01)00291-5).
- [11] Hamdeh N, Muhtaseb M. Optimization of solar adsorption refrigeration system using experimental and statistical techniques. *Energy Convers. Manag.* 2010;51:1610–1615. <https://doi.org/10.1016/j.enconman.2009.11.048>.
- [12] Deshmukh H, Maiya MP, Murthy SS. Continuous vapour adsorption cooling system with three adsorber beds. *Appl. Therm. Eng.* 2015;82:380–389. <https://doi.org/10.1016/j.applthermaleng.2015.01.013>.
- [13] Sur A, Das RK. Development of equilibrium and dynamic models for an adsorption refrigeration system. *J. environ. biotechnol. res.* 2017;6:64–81.
- [14] Sheikholeslami M, Ul-Haq R, Shafee A, Li Z. Heat transfer behaviour of nanoparticle enhanced PCM solidification through an enclosure with V shaped fins.

- Int J Heat Mass Transf 2019;130:1322-1342. <https://doi.org/10.1016/j.ijheatmasstransfer.2018.11.020>.
- [15] Sheikholeslami M, Ul Haq R, Shafee A, Li Z. Heat transfer simulation of heat storage unit with nanoparticles and fins through a heat exchanger. *Int J Heat Mass Transf* 2019;135:470–478. <https://doi.org/10.1016/j.ijheatmasstransfer.2019.02.003>.
- [16] Dixit M, Arora A, Kaushik SC. Energy and exergy analysis of a waste heat driven cycle for triple effect refrigeration. *J. Therm. Eng.* 2016;2:954–961. <https://doi.org/10.18186/jte.84533>.
- [17] Javadi MA, Hoseinzadeh S, Ghasemiasl R, Heyns PS, Chamkha AJ. Sensitivity analysis of combined cycle parameters on exergy, economic, and environmental of a power plant. *J Therm Anal Calorim* 2019;139:519–525. <https://doi.org/10.1007/s10973-019-08399-y>.
- [18] Sheikholeslami M, Ul Haq R, Shafee A, Jafaryar M, Li Z. Heat transfer of nanoparticles employing innovative turbulator considering entropy generation, *Int J Heat Mass Transf* 2019;136:1233–1240. <https://doi.org/10.1016/j.ijheatmasstransfer.2019.03.091>.
- [19] Sheikholeslami M, Ul Haq R, Shafee A, Jafaryar M, Li Z. Heat transfer and turbulent simulation of nanomaterial due to compound turbulator including irreversibility analysis, *Int J Heat Mass Transf*. 2019;137:1290–1300. <https://doi.org/10.1016/j.ijheatmasstransfer.2019.04.030>.
- [20] Kurtulmus N, Bilgili M, Şahin B. Energy and Exergy Analysis of a Vapor Absorption Refrigeration System in an Intercity Bus Application. *J. Therm. Eng.* 2019;4:355–371. <https://doi.org/10.18186/thermal.583316>.
- [21] Kalla S, Arora B, Usmani J. Performance Analysis of R22 and its Substitutes in Air Conditioners. *J. Therm. Eng.* 2018;4:1724–1736. <https://doi.org/10.18186/journal-of-thermal-engineering.367419>.
- [22] Javadi MA, Hoseinzadeh S, Ghasemiasl R, Khalaji M. Optimization and analysis of exergy, economic, and environmental of a combined cycle power plant, *Sadhana Ind. Acad. of Scien.* 2019;5:1–11. <https://doi.org/10.1007/s12046-019-1102-4>.
- [23] Anand Y, Gupta A, Tyagi S, Anand S. Variable Capacity Absorption Cooling System Performance for Building Application, *J. Therm. Eng.* 2018;4:2303–2317. <https://doi.org/10.18186/thermal.439041>.
- [24] Bhargav H, Ramani B, Reddy VS, Lai F. Development of semi-continuous solar powered adsorption water chiller for food preservation, *J. Therm. Eng.* 2018;4:2169–2187. <https://doi.org/10.18186/journal-of-thermal-engineering.434032>.
- [25] El-Sharkawy II, Pal A, Miyazaki T, Saha BB, Koyama S. A study on consolidated composite adsorbent for cooling application. *Appl. Therm. Eng.* 2016;98:1214–1220. <https://doi.org/10.1016/j.applthermaleng.2015.12.105>.
- [26] Oertel K, Fischer M. Adsorption cooling system for cold storage using methanol/silica-gel. *Appl. Therm. Eng.* 1998;18:773–786. [https://doi.org/10.1016/S1359-4311\(97\)00107-5](https://doi.org/10.1016/S1359-4311(97)00107-5).
- [27] Buzanowski MA, Yang RT. Extended linear driving-force approximation for intraparticle diffusion rate including short times. *Chem. Eng. Sci.* 1989;44:2683–2689. [https://doi.org/10.1016/0009-2509\(89\)85211-X](https://doi.org/10.1016/0009-2509(89)85211-X).
- [28] Sur A, Das RK. Numerical modeling and thermal analysis of an adsorption refrigeration system, *Int J. Air-Cond. Ref.* 2015;23:1550033. <https://doi.org/10.1142/S2010132515500339>.